Molecular Basis of the Medium-Chain Fatty Acyl-CoA Dehydrogenase-Catalyzed "Oxidase" Reaction: pH-Dependent Distribution of Intermediary Enzyme Species during Catalysis†

Jeffrey K. Johnson, N. Ravi Kumar, and D. K. Srivastava*

Biochemistry Department, North Dakota State University, Fargo, North Dakota 58105

Received October 27, 1993; Revised Manuscript Received February 14, 1994®

ABSTRACT: In a previous paper, we demonstrated that the medium-chain fatty acyl-CoA dehydrogenase-catalyzed (MCAD-catalyzed) reductive half-reaction of indolepropionyl-CoA proceeds via formation of a chromophoric intermediary species "X" (absorption maximum = 400 nm) and proposed that the decay of this species might limit the overall rate of the "oxidase" reaction [Johnson, J. K., & Srivastava, D. K. (1993) *Biochemistry 32*, 8004–8013]. During this latter reaction, the buffer-dissolved O_2 served as an electron acceptor [Johnson, J. K., Wang, Z. X., & Srivastava, D. K. (1992) *Biochemistry 31*, 10564–10575]. To ascertain whether the intrinsic stability of X influences the oxidase activity, we undertook a detailed kinetic investigation of this enzyme at different pH values. The time-resolved spectra for the reductive half-reaction (obtained via the rapid-scanning stopped-flow method) at different pH values reveal that the amplitude of the intermediary (X) spectral band is more pronounced at a lower pH (pH 6.4) than at a higher pH (pH 9.0). Single-wavelength transient kinetic data for the reductive half-reaction (in both the forward and the reverse direction) at all pH values are consistent with fast ($1/\tau_1$) and slow ($1/\tau_2$) relaxation rate constants. Of these, whereas the fast relaxation rate constant for the reaction in the forward direction ($1/\tau_{1f}$) decreases with an increase in pH, the corresponding slow relaxation rate constant ($1/\tau_{2f}$) increases with an increase in pH. The pH-dependent steady-state kinetic data reveal that, like $1/\tau_{2f}$, k_{cat} for the MCAD-catalyzed oxidase reaction increases with an increase in the pH of the buffer media. These results coupled with the substrate and product concentration-dependent relaxation studies (both in the forward and the reverse direction) as well as the direct measurements of the rate constants of E–$FADH_2$ oxidation at different pH values lead us to conclude the following: (1) The catalytic efficiency of the oxidase reaction is primarily determined by the forward rate constant for the conversion of X to the E–$FADH_2$–P complex. (2) The increase in pH destabilizes the intermediary species X by promoting its distribution toward both the E–FAD–S and the E–$FADH_2$–P complex. (3) There is no discernible effect of pH on the rate of oxidation of E–$FADH_2$ by the buffer-dissolved O_2. (4) The steady-state kinetic parameters for the oxidase reaction are predictable by the microscopic rate constants of the overall enzyme-catalyzed reaction at different pH values. The effector role of the substrate and/or the pH responsible for the origin of the oxidase activity during the MCAD catalysis is discussed.

The medium-chain fatty acyl-CoA dehydrogenase-catalyzed (MCAD[1] -catalyzed) reaction proceeds via a concerted abstraction of a proton and a hydride ion from the α- and β-carbons, respectively, of fatty acyl-CoA chains, concomitant with the reduction of the MCAD-bound FAD to $FADH_2$ [for reviews, see Beinert (1963) and Engel (1990)]. The repetitive turnover of the enzyme under physiological conditions is believed to be maintained by transfer of electrons from MCAD–$FADH_2$ to the electron-transferring flavoprotein (ETF)–FAD (Crane & Beinert, 1956; Ghisla & Massey, 1989). Due to a variety of spectroscopic signals associated with both flavin cofactor and the chromophoric acyl-CoA substrates, this enzyme has been a subject of intense mechanistic investigation in recent years (Frerman et al., 1980; McFarland et al., 1982; Ghisla et al., 1984; Lau et al., 1989). By utilizing indolepropionyl/indoleacryloyl-CoA as the chromophoric substrate/product pair (eq 1), we have elaborated on certain aspects of ligand-binding and reductive and oxidative half-reactions of this enzyme (Johnson et al., 1992, 1993; Johnson & Srivastava, 1993).

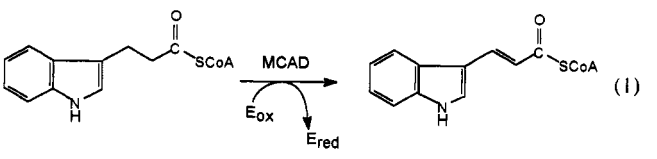

Due to a characteristic absorption band of the reaction product, indoleacryloyl-CoA (absorption maximum = 367 nm), we could monitor the (steady state) time course of the enzyme-catalyzed reaction without recourse to the signals of external electron acceptors (Johnson et al., 1992). In this way, we observed that the MCAD-catalyzed reaction proceeds via two pathways: (A) a "dehydrogenase" pathway which predominates in the presence of a variety of "organic" electron acceptors such as ETF/DCPIP, $FcPF_6$, and others and (B) an "oxidase" pathway in which the buffer-dissolved O_2

† Journal article no. 2148 of the North Dakota Agricultural Experiment Station. Supported by the American Heart Association, Dakota Affiliate.

* To whom correspondence should be addressed: Biochemistry Department, North Dakota State University, Fargo, ND 58105.

® Abstract published in *Advance ACS Abstracts*, April 1, 1994.

[1] Abbreviations: MCAD, medium-chain fatty acyl-CoA dehydrogenase; IPCoA, 3-indolepropionyl coenzyme A; IACoA, *trans*-3-indoleacryloyl coenzyme A; $FcPF_6$, ferrocenium hexafluorophosphate; FAD, flavin adenine dinucleotide; $FADH_2$, reduced flavin adenine dinucleotide; EDTA, ethylenediaminetetraacetic acid; RSSF, rapid-scanning stopped-flow; E_{ox}, oxidized form of the electron acceptor; E_{red}, reduced form of the electron acceptor.

0006-2960/94/0433-4738$04.50/0

exclusively acts as an electron acceptor. The steady-state kinetic investigation for these reactions revealed that the K_m (for IPCoA) and the k_{cat} for the dehydrogenase reaction were about 1 order of magnitude higher than those for the oxidase reaction (Johnson et al., 1992). This observation led us to suspect that the microscopic pathways for the dehydrogenase and the oxidase reactions might be different.

Transient kinetic investigations into the mechanism of the MCAD-catalyzed reductive half-reaction allowed us, as well as other investigators, to delineate the sequence of events during the single turnover of the enzyme (Johnson & Srivastava, 1993; Schopfer et al., 1988). Utilizing indolepropionyl-CoA as a substrate, we demonstrated that the reductive half-reaction proceeds via formation of an intermediary species, "X", that is characterized by a unique absorption band at 400 nm (Johnson & Srivastava, 1993). The time course for the formation and decay of X was found to be similar to the appearance and disappearance of the charge-transfer complex band at 600 nm (Johnson & Srivastava, 1993). By transient kinetic methods, we determined all of the microscopic constants for the reductive half-reaction of this enzyme at pH 7.6. A casual perusal of these parameters vis-à-vis the steady-state kinetic parameters for the dehydrogenase-catalyzed (K_m(IPCoA) = 10.3 μM, k_{cat} = 0.46 s^{-1}) and oxidase catalyzed reactions (K_m(IPCoA) = 0.49 μM, k_{cat} = 0.016 s^{-1}) (Johnson et al., 1992) allowed us to propose that the rate-limiting step for the dehydrogenation reaction might be the formation of X (0.57 s^{-1}), whereas that for the oxidase reaction might be the decay of X (0.01 s^{-1}) (Johnson & Srivastava, 1993).

The MCAD-catalyzed oxidase reaction is not novel to the use of IPCoA as the enzyme substrate. A number of previous investigators have noted oxidase activity of this enzyme by utilizing a variety of CoA substrates (McFarland et al., 1982; Schopfer et al., 1988; Wang & Thorpe, 1991). Recently, Vanhove et al. (1993) have demonstrated that an analogous enzyme, short-chain fatty acyl-CoA dehydrogenase, catalyzes the oxidase reaction involving a variety of fatty acyl-CoA substrates.

It should be pointed out that the oxidase activity of the enzyme usually remains elusive with aliphatic-CoA substrates (due to the colorless form of their corresponding enoyl-CoA products) unless special efforts are made (McFarland et al., 1982; Vanhove et al., 1993). Such efforts include assay conditions designed to detect the reduced oxygen species, viz., hydrogen peroxide (McFarland et al., 1982; Wang & Thorpe, 1991), superoxide anion (Nishino et al., 1989), and others. This is presumably the reason why the enzyme-catalyzed oxidase reaction has not been seriously investigated. To the best of our knowledge, we have been the first to propose that the MCAD-catalyzed oxidase reaction exhibits a Michaelian dependence on its substrate concentration (Johnson et al., 1992).

Our interest in the MCAD-catalyzed oxidase reaction emerged from the mechanistic as well as the structural–functional point of view (Johnson et al., 1992). Given that the pH influences the isomerization equilibrium between the E–FAD–IACoA and E–FAD*–IACoA** complexes (Johnson et al., 1992), it occurred to us that pH might affect the distribution between X and the E–$FADH_2$–IACoA complex during the reductive half-reaction (Johnson & Srivastava, 1993) and thus would effect the oxidase activity of the enzyme. The experimental results presented below clearly substantiate these expectations.

MATERIALS AND METHODS

Materials. Coenzyme A, glucose oxidase (type VII), and EDTA were purchased from Sigma. 3-Indolepropionic acid and *trans*-3-indoleacrylic acid, used in the synthesis of substrates, were purchased from Aldrich. All other reagents were of analytical reagent grade.

Methods. The CoA derivatives of 3-indolepropionic acid (IPCoA) and *trans*-3-indoleacrylic acid (IACoA) were synthesized and purified according to Johnson et al. (1992). Medium-chain fatty acyl-CoA dehydrogenase (MCAD) was purified in our laboratory as described previously (Johnson et al., 1992).

MCAD was routinely assayed in 50 mM potassium phosphate buffer (pH 7.6) containing 0.3 mM EDTA at 25 °C, utilizing 30 μM octanoyl-CoA and 200 μM ferrocenium hexafluorophosphate ($FcPF_6$) as described by Lehman et al. (1990). The active enzyme concentration was determined in terms of the flavin content by using an extinction coefficient of 15.4 mM^{-1} cm^{-1} at 446 nm (Thorpe et al., 1979). IPCoA and IACoA concentrations were determined using extinction coefficients of 18.2 mM^{-1} cm^{-1} at 259 nm and 26.5 mM^{-1} cm^{-1} at 367 nm, respectively (Johnson et al., 1992). Experiments involving pH effects were performed in the following buffers: for pH ranges between 6 and 8, 50 mM potassium phosphate containing 0.3 mM EDTA was used; for pH ranges between 8 and 10.5, 0.1 M Tris-HCl plus 50 mM potassium phosphate buffer containing 0.3 mM EDTA was used.

Steady-state kinetics for the enzyme-catalyzed oxidase reaction was performed on a Perkin Elmer Lambda 3B spectrophotometer, utilizing a 10-cm-path-length cuvette. Other experiments and data analyses were performed as described by Johnson and Srivastava (1993) and Johnson et al. (1993). Single-wavelength transient kinetic studies and data analysis were performed on an Applied Photophysics MV-14 sequential-mixing stopped-flow system (optical path length = 1 cm; dead time = 1.34 ms). The time-resolved spectra were acquired on a Durrum stopped-flow system (optical path length = 1.5 cm; dead time = 3–5 ms), configured in our laboratory as a rapid-scanning device (Johnson & Srivastava, 1993).

Oxidation of MCAD–$FADH_2$ by O_2. MCAD–$FADH_2$ was generated by incubation of MCAD–FAD with sodium dithionite in an appropriate anaerobic buffer (at different pH). The anaerobic buffers used for these experiments were prepared by a repeated cycle of degassing and purging with oxygen-free argon. Since these buffers did not contain glucose and glucose oxidase to scavenge the residual traces of oxygen, a higher concentration of sodium dithionite (about 50–70 μM) was required for a quantitative reduction of the enzyme. The amount of sodium dithionite required to reduce a fixed concentration of MCAD–FAD was predetermined by measuring the absorption at 450 nm. Oxygen concentration in different buffers was adjusted by mixing an appropriate ratio of anaerobic buffer (prepared as described above) and fully oxygenated buffer. The final concentration of oxygen in the buffer was determined by Yellow Spring Instrument (YSI) biological oxygen monitor (Model 5300).

The time-dependent increase in absorption at 450 nm was monitored upon mixing of sodium dithionite-reduced MCAD and (buffer-dissolved) oxygen via the stopped-flow syringes. The concentrations of enzyme and oxygen (after mixing) were 5 and 240 μM, respectively, at different pH values. The reaction profiles were analyzed according to a single-exponential rate law. At pH 7.6, we measured the rates of oxidation of the reduced enzyme at different concentrations

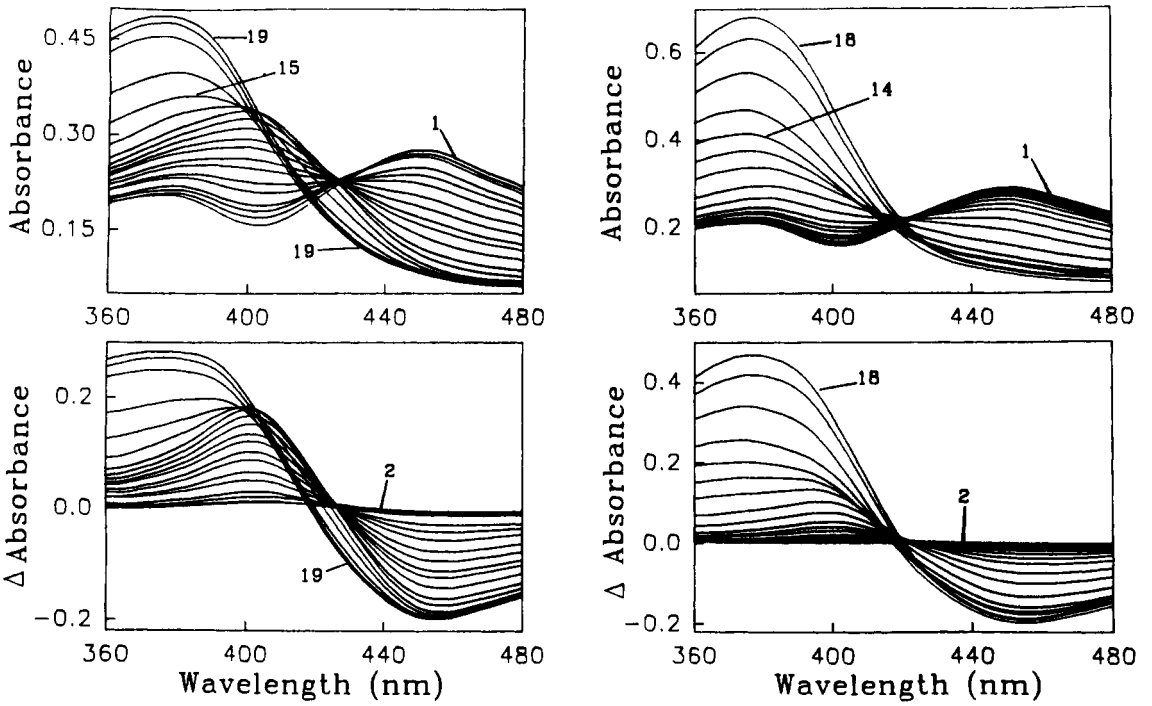

FIGURE 1: Rapid-scanning stopped-flow spectra for the reaction of MCAD–FAD with IPCoA ([IPCoA] ≫ [MCAD–FAD]) at pH 6.4 (left panels) and 9.0 (right panels) under anaerobic conditions. The concentrations of MCAD–FAD (syringe 1) and IPCoA (syringe 2) prior to mixing were 20 and 200 μM, respectively. The top and bottom panels show normal spectra and difference spectra (spectra at given times minus the first spectrum) at the corresponding pH values. The time delays (in seconds) for the spectral traces (1–20) in the left panels (pH 6.4) were as follows: 0, 0.034, 0.052, 0.069, 0.138, 0.224, 0.31, 0.48, 0.654, 0.895, 1.08, 1.51, 2.37, 4.1, 11.9, 24.8, 51.5, 138, 241, and 282. The time delays (in seconds) for the traces (1–18) in the right panels (pH 9.0) were as follows: 0, 0.026, 0.052, 0.138, 0.224, 0.31, 0.48, 0.654, 0.895, 1.51, 2.37, 4.1, 6.28, 9.26, 14.5, 103, 241, and 282.

of buffer-dissolved oxygen. The data were analyzed for a linear dependence of the observed rate constant as a function of the oxygen concentration. The slope of this plot was taken as a measure of the second-order rate constant.

RESULTS

Having surmised that pH might influence the equilibrium distribution of the intermediary species (see the introduction), we undertook a pH-dependent transient kinetic study of the reductive half-reaction of the medium-chain fatty acyl-CoA dehydrogenase (MCAD) utilizing indolepropionyl-CoA (IPCoA) as a chromophoric substrate. In this pursuit, we compared the time-resolved spectral changes (acquired via the rapid-scanning stopped-flow, or RSSF, method) at selected pH values (viz., pH 6.4, 7.6, and 9.0). Figure 1 shows the RSSF spectra for the reaction of MCAD–FAD with IPCoA (after-mixing concentrations of 10 and 100 μM, respectively) under anaerobic conditions at pH 6.4 and 9.0, respectively. Although the timing sequences for different spectral traces are more or less the same, the spectral patterns at these two pH values are remarkably different. The most noticeable difference is the amplitude of the intermediary spectral band at 400 nm (due to the formation of X; Johnson & Srivastava, 1993). This band is more pronounced at pH 6.4 than at pH 9.0. This feature is further explicit in the difference spectra (i.e., the spectra at given times minus the first spectrum) of Figure 1 (bottom panels). The spectral pattern obtained at pH 6.4 was found to be similar to that observed at pH 7.6 (data not shown).

Given that pH influences the electronic spectrum of neither E–FAD nor IACoA (Johnson et al., 1992), the pronounced spectral band (at 400 nm) at pH 6.4 vis-à-vis that at pH 9.0 can be envisaged to originate from some pH-dependent changes in the kinetic and/or the thermodynamic properties of the

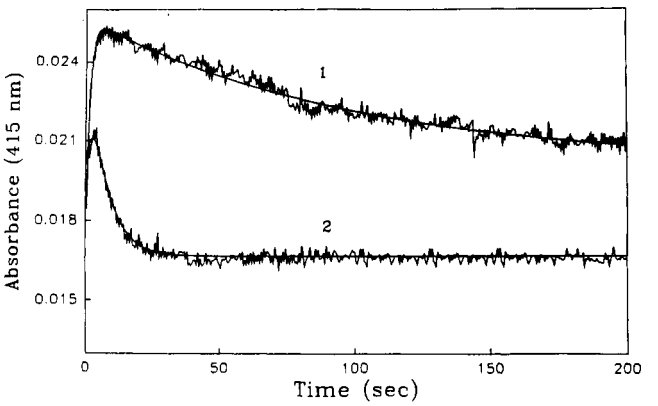

FIGURE 2: Single-wavelength (415 nm) stopped-flow traces (trace 1 at pH 6.4, trace 2 at pH 9.0) for the reaction of 2.4 μM MCAD–FAD (syringe 1) and 200 μM IPCoA (syringe 2). Solid lines are the best fits of the experimental data according to the two-exponential rate equations (for increasing and decreasing phase). The relaxation rate constants for the fast ($1/\tau_{1f}$) and slow ($1/\tau_{2f}$) phases are 1.03 and 0.0083 s^{-1} at pH 6.4 and 0.45 and 0.16 s^{-1} at pH 9.0, respectively.

enzyme. To ascertain whether the amplitude of the intermediary spectral band (X) is kinetically controlled, we performed a single-wavelength stopped-flow study (under anaerobic conditions) for the reaction of MCAD–FAD and IPCoA at pH 6.4 and 9.0, utilizing a lower concentration of the enzyme. Figure 2 shows the time course of the absorption changes at 415 nm upon mixing MCAD–FAD with IPCoA (after-mixing concentrations of 1.2 μM and 100 μM, respectively) via the stopped-flow syringes. Note that at pH 6.4 a rapid increase in absorption (at 415 nm) follows a slow decrease. This pattern is different from that observed at pH 9.0. At the latter pH, a somewhat slower rate of increase in absorption is followed by a rapid decrease. Upon analyzing these kinetic traces by a two-exponential rate equation, we

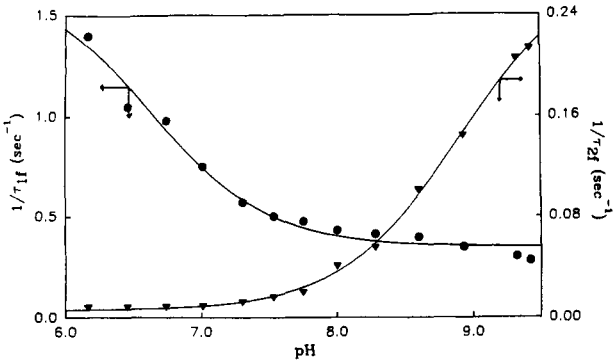

FIGURE 3: pH-dependent changes in the fast ($1/\tau_{1f}$) and slow ($1/\tau_{2f}$) relaxation rate constants for the reaction of 2.4 μM MCAD–FAD (syringe 1) and 200 μM IPCoA. The magnitudes of $1/\tau_{1f}$ and $1/\tau_{2f}$ were obtained from the best fits of the experimental data at 400 and 415 nm, respectively. Note that as pH increases, $1/\tau_{1f}$ and $1/\tau_{2f}$ decrease and increase, respectively. The solid lines are the best fits of the experimental data according to the Henderson–Hasselbalch equation with pK_a values equal to 6.63 ± 0.10 (from the data of the $1/\tau_{1f}$ versus pH plot) and 8.90 ± 0.03 (from the data of the $1/\tau_{2f}$ versus pH plot).

determined the fast ($1/\tau_{1f}$, increasing phase; the "f" in the subscript stands for the reaction in the forward direction) and slow ($1/\tau_{2f}$, decreasing phase) relaxation rate constants to be 1.03 and 0.008 s^{-1} at pH 6.4 and 0.45 and 0.16 s^{-1} at pH 9.0, respectively. These results coupled with the fact that the amplitude of the absorption changes is higher at pH 6.4 than at pH 9.0 suggest that the equilibration rate leading to the formation of X is faster than that leading to its decay at pH 6.4. Hence, the higher amplitude of the intermediary absorption band at 400 nm (at pH 6.4) is clearly due to a rapid production of X followed by its slow decay.

The time courses for the absorption changes at most of the wavelengths (except at isoabsorption points) are consistent with two-exponential processes (increase, decrease, or a combination of the two) corresponding to the relaxation rate constants $1/\tau_{1f}$ and $1/\tau_{2f}$, respectively (Johnson & Srivastava, 1993). To ascertain the influence of pH on these relaxation rate constants, we performed experiments similar to that presented in Figure 2 at different pH values. The concentrations of E–FAD and IPCoA (after mixing) were maintained at 1.2 and 100 μM, respectively, in the stopped-flow syringes for all pH-dependent experiments. For convenience, the magnitudes of $1/\tau_{1f}$ and $1/\tau_{2f}$ were calculated from the best fit of the experimental data at wavelengths of 400 and 415 nm, respectively. As noted by us previously, $1/\tau_{1f}$ calculated from the data at 415 nm was the same as that calculated at 400 nm (Johnson & Srivastava, 1993).

Figure 3 shows the pH-dependent variations in $1/\tau_{1f}$ and $1/\tau_{2f}$. It is noteworthy that $1/\tau_{1f}$ sharply decreases with increasing pH over the pH range 6.2–7.0, and after that it becomes constant. This is in marked contrast to the dependence of $1/\tau_{2f}$ on pH. The magnitude of $1/\tau_{2f}$ remains invariant with increasing pH over the pH range 6.2–7.0, and after that it starts increasing rather sharply. From the best fit of the experimental data according to the Henderson–Hasselbalch equation, we have determined the pK_a values of 6.63 ± 0.10 and 8.90 ± 0.03 from the data of $1/\tau_{1f}$ and $1/\tau_{2f}$, respectively. It should be pointed out that these pK_a's have no physical meaning with regard to the dissociability of specific active site groups. Rather, they are a complex function of the various pH-dependent processes. From the data of Figure 3, it is noteworthy that the ratio of $1/\tau_{1f}$ and $1/\tau_{2f}$ decreases from 177 at pH 6.2 to 1.3 at pH 9.4. Although the pH-dependent variation of this ratio is not a quantitative measure

Table 1: Summary of $1/\tau_{max}$, $1/\tau_{min}$ and $K_{0.5}$ Values Derived from the Dependence of Relaxation Rate Constants on IPCoA/IACoA Concentrations at Different pH Values

	pH		
	6.4	7.6	9.0
IPCoA			
$1/\tau_{1f(max)}$ (s^{-1})	1.32	0.63	0.69
$1/\tau_{1f(min)}$ (s^{-1})	0.03	0.08	0.12
$1/\tau_{2f(min)}$ (s^{-1})	0.005	0.01	0.11
$K_{0.5}$ (μM)	11.5	11.5	11.2
IACoA			
$1/\tau_{1r(max)}$ (s^{-1})	1.99	4.38	12.90
$1/\tau_{1r(min)}$ (s^{-1})	0.005	0.01	1.43
$1/\tau_{2r(min)}$ (s^{-1})	0.03	0.08	0.04
$K_{0.5}$ (μM)	23.7	14.9	6.4

of the equilibrium distribution among the various forms of the enzyme species, it provides some indication as to the distribution of the enzyme species among E–FAD–IPCoA, X, and E–FADH$_2$–IACoA complexes. A higher ratio of $1/\tau_{1f}$ and $1/\tau_{2f}$ at lower pH values attests to the fact that the microscopic steps intrinsic to $1/\tau_{1f}$ are not intimately coupled to those with $1/\tau_{2f}$ (Bernasconi, 1976). This is clearly not the case under conditions (i.e., at higher pH values) where the magnitudes of $1/\tau_{1f}$ and $1/\tau_{2f}$ are comparable (see Discussion).

We performed the IPCoA concentration dependent relaxation studies for the reaction of E–FAD + IPCoA (under condition where [IPCoA] ≫ [E–FAD]) at pH values 6.4, 7.6, and 9.0. As observed by us previously (Johnson & Srivastava, 1993), at all these pH values, $1/\tau_{1f}$ increases hyperbolically (with an offset) with an increase in IPCoA concentration. On the contrary, $1/\tau_{2f}$ decreases with an increase in IPCoA concentration. These data were analyzed essentially as described by Johnson and Srivastava (1993), except the magnitude of the "offset" was set equal to the slow relaxation rate constant in the reverse direction ($1/\tau_{2r}$) at a saturating concentration of IACoA. This strategem minimized the error introduced by extrapolation of $1/\tau_{1f}$ to zero concentration of IPCoA. The magnitudes of $1/\tau_{1f}$ at zero (offset) and saturating (asymptote) concentrations of IPCoA are taken to be the measures of the maximum ($1/\tau_{1f(max)}$) and minimum ($1/\tau_{1f(min)}$) relaxation rate constants. The concentrations of IPCoA required to attain one-half of the total changes are represented by $K_{0.5}$. These values are given in Table 1. We have not rigorously analyzed, at this time, the (decreasing) hyperbolic dependence of $1/\tau_{2f}$ on [IPCoA], except for determining its magnitude at saturating concentrations of the latter. Under these conditions, $1/\tau_{2f}$ attains a minimum value and is represented by $1/\tau_{2f(min)}$ (Table 1) at different pH's.

We performed analogous transient kinetic experiments for the reaction in the reverse direction, i.e., between E–FADH$_2$ (generated by sodium dithionite reduction) and IACoA. The time courses for the reaction of 2 μM E–FADH$_2$ and varying concentrations of IACoA ([IACoA] > [E–FADH$_2$]) were measured at 415 nm, at selected pH values. Like the reaction profiles in the forward direction, the reverse reaction profiles were consistent with two relaxation rate constants, $1/\tau_{1r}$ and $1/\tau_{2r}$ ("r" denotes the reaction in the reverse direction), and showed hyperbolic increasing and decreasing dependence on IACoA concentrations, respectively. These data were analyzed as described above, and the magnitudes of $1/\tau_{1r(max)}$, $1/\tau_{1r(min)}$, $1/\tau_{2r(min)}$, and $K_{0.5}$ were determined (Table 1). The experimental data of Table 1 have been used to calculate the microscopic parameters for the overall reductive half-reaction at different pH values (see Table 3, and Discussion).

Steady-State Kinetics for the Oxidase Reaction. We performed the steady-state kinetics for the MCAD-catalyzed

Table 2: Steady-State Kinetic Parameters for the MCAD-Catalyzed Oxidase Reaction

	experimentally determined		predicted[a]	
pH	K_m(IPCoA) (μM)	k_{cat} (s^{-1})	K_m(IPCoA) (μM)	k_{cat} (s^{-1})
6.4	0.21 ± 0.017	0.008 ± 0.0002	0.30	0.005
7.6	0.49 ± 0.040	0.016 ± 0.0004	1.60	0.008
9.0	0.79 ± 0.085	0.038 ± 0.0014	3.25	0.046

[a] According to eqs 5A and 5B, utilizing the microscopic parameters of Table 3.

Table 3: Microscopic Parameters for the MCAD-Catalyzed Reductive Half-Reaction at Different pH Values

	pH		
	6.4	7.6	9.0
K_s (μM)	11.5	11.5	11.2
k_2 (s^{-1})	1.29	0.55	0.50
k_{-2} (s^{-1})	0.03	0.08	0.15
k_3 (s^{-1})	0.005	0.010	0.070
k_{-3} (s^{-1})	1.99	4.38	12.79
K_p (μM)	23.70	14.90	6.40
k_5 (s^{-1})	0.97	1.03	1.00

oxidase reaction utilizing IPCoA as the enzyme substrate. Due to a low K_m value for IPCoA during the oxidase reaction, these experiments were performed in a 10-cm-path-length cuvette. The initial rates of the enzyme-catalyzed conversion of IPCoA to IACoA were measured at 367 nm, in the absence of any externally added organic electron acceptors. The initial rate of the enzyme-catalyzed reaction showed a Michaelian dependence on IPCoA concentration at all the pH values examined (i.e., pH 6.4, 7.6, and 9.0). From the best fit of the experimental data according to the Michaelis–Menten equation, the K_m(IPCoA) and k_{cat} for the oxidase reaction were calculated at these pH values (Table 2). Although we have not determined whether the buffer-dissolved oxygen (240 μM) is saturating for the IPCoA-dependent oxidase reaction, the K_m for oxygen during the enzyme-catalyzed oxidation of indolepropionyl pantetheine phosphate (3′,5′-ADP truncated IPCoA) to indoleacryloyl pantetheine phosphate is about 28 μM (our unpublished results). However, the steady-state parameters are still considered to be "apparent" since they have not been obtained by extrapolation of initial rates at infinite concentrations of O_2.

From this limited experimental data, it is evident that as the pH increases both k_{cat} and K_m(IPCoA) increase (Table 2). Given that the K_m for IPCoA at all these pH values (Table 2) is less than 1 μM, we measured the turnover number of the MCAD-catalyzed oxidase reaction at different pH values (ranging from pH 6.0 to 10.5) in the presence of a saturating (50 μM) concentration of IPCoA (Figure 4). It is noteworthy that the turnover rate (k_{cat}) for the MCAD-catalyzed oxidase reaction remains more or less constant over the pH range 5.8–7.8, but it starts increasing (rather sharply) beyond the latter pH value. This pattern is analogous to the dependence of $1/\tau_{2f}$ on pH (see Figure 3). The pH-dependent oxidase reaction is consistent with a pK_a of 9.91 ± 0.05. This pK_a is 1 unit higher than that observed for the dependence of $1/\tau_{2f}$ on pH. This discrepancy is presumably due to the fact that the oxidase reaction is primarily limited by the forward rate constant for the decay of X, whereas $1/\tau_{2f}$ is a combined function of the various microscopic rate constants (see Discussion).

Oxidation of MCAD-Bound $FADH_2$ by Buffer-Dissolved O_2. To provide a detailed molecular basis for the MCAD-catalyzed oxidase reaction, we decided to determine the rate

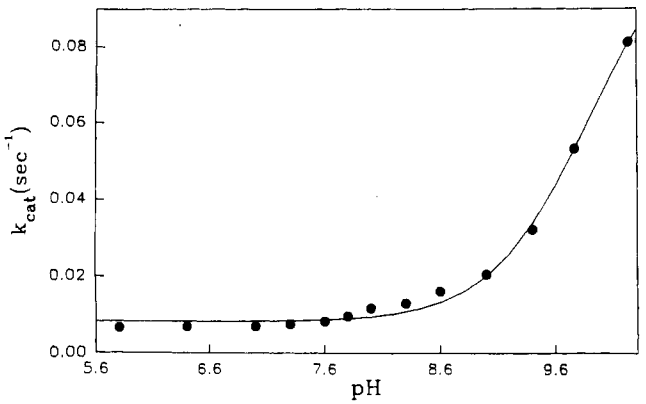

FIGURE 4: Effect of pH on the turnover rate (k_{cat}) for the MCAD-catalyzed oxidase reaction in the presence of buffer-dissolved O_2 (240 μM). The concentrations of the enzyme and IPCoA were 0.77 and 50 μM, respectively. The solid line is the best fit of the experimental data according to the Henderson–Hasselbalch equation with a pK_a of 9.91 ● 0.05.

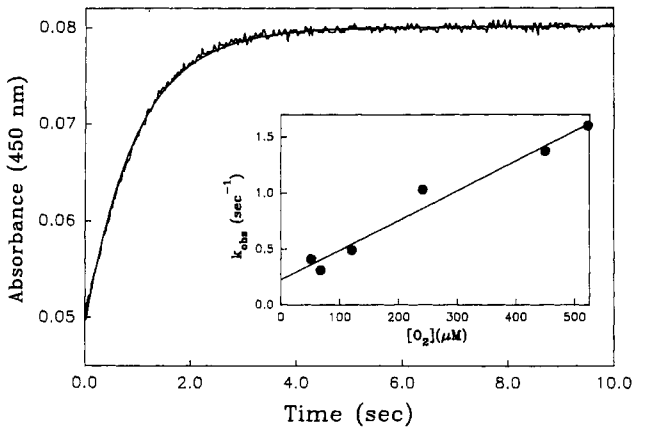

FIGURE 5: Reaction of MCAD–$FADH_2$ with buffer-dissolved oxygen at pH 7.6. The time-dependent change in the absorption at 450 nm for the reaction of 10 μM MCAD–$FADH_2$ (syringe 1) and 480 μM buffer-dissolved oxygen is shown (the after-mixing concentrations of enzyme and oxygen are 5.0 and 240 μM, respectively). The solid line is the best fit of the experimental data according to the single-exponential (increase) rate equation, for a rate constant of 1.03 s^{-1}. The inset shows the effect of oxygen concentration on the observed rate constant for the MCAD–$FADH_2$ oxidation. The solid line is the best fit of the experimental data, with a second-order rate constant of (2.65 ± 0.23) × 10^3 M^{-1} s^{-1}.

constant for the MCAD–$FADH_2$ oxidation by the buffer-dissolved oxygen at selected pH values. This experiment was performed by mixing sodium dithionite-reduced enzyme (10 μM) with an oxygen-saturated buffer (oxygen concentration = 480 μM) in the stopped-flow syringes (see Materials and Methods). In this way, the after-mixing concentration of oxygen was maintained at 240 μM (similar to the concentration of the buffer-dissolved oxygen under normal conditions). The time courses for the oxidation of MCAD–$FADH_2$, at different pH values, by (240 μM) buffer-dissolved oxygen were monitored at 450 nm. Figure 5 shows a representative trace for the oxidation of MCAD–$FADH_2$ at pH 7.6. From the best fit of the experimental data according to a single-exponential rate law (solid line), we have determined the first-order constant for the oxidation of E–$FADH_2$ by O_2 to be 1.03 s^{-1} (at pH 7.6). The corresponding rate constants at pH 6.4 and 9.0 (under identical experimental conditions) were found to be 0.97 and 1.0 s^{-1}, respectively.

We measured the rate of oxidation of MCAD–$FADH_2$ at different concentrations of the buffer-dissolved oxygen at pH 7.6. The oxygen concentration during these experiments was

maintained to satisfy pseudo-first-order conditions. The data were analyzed for a single-exponential increase in absorption at all oxygen concentrations. The inset of Figure 5 shows a linear dependence of the observed rate constant (k_{obs}) as a function of oxygen concentration, suggesting that the overall oxidation reaction is a second-order process. The slope of this plot [$(2.65 \pm 0.23) \times 10^3$ M^{-1} s^{-1}] is taken to be a measure of the second-order rate constant for the oxidation of MCAD–$FADH_2$ by oxygen at pH 7.6.

DISCUSSION

The pH-dependent investigation presented herein has been prompted by our realization that there is an intrinsic commonality between the microscopic pathways leading to E–FAD + IACoA interaction and E–FAD/$FADH_2$ + IPCoA/IACoA binding followed by chemical transformations (eq 2).

$$\text{E–FAD} + \text{IACoA} \rightleftharpoons \text{E–FAD–IACoA} \rightleftharpoons \text{E–FAD*–IACoA**} \quad (2A)$$

$$\text{E–FAD} + \text{IPCoA} \rightleftharpoons \text{E–FAD–IPCoA} \rightleftharpoons \text{X (E–FADH}_2\text{–IACoA*)} \quad (2B)$$

$$\text{E–FADH}_2 + \text{IACoA} \rightleftharpoons \text{E–FADH}_2\text{–IACoA} \rightleftharpoons \text{X (E–FADH}_2\text{–IACoA*)} \quad (2C)$$

Both of these processes occur in two steps. The first (fast) step involves the formation of a collision complex between the enzyme and the CoA derivative. This complex is slowly isomerized to a more stable complex during the second step. This two-step binding and/or catalysis has been observed not only with these chromophoric substrates but also with butyryl-crotonoy-CoA and octanoyl-octenoyl-CoA pairs, and even in the case of the E–FAD + acetoacetyl-CoA interaction (our unpublished results). The only difference between these two seemingly diverse phenomena is that the slow steps of eqs 2A and 2C are devoid of "chemistry", whereas that of eq 2B is coupled to the oxidation/reduction reaction.

The RSSF data, coupled with the single-wavelength stopped-flow studies, at different pH values substantiate that the intermediary species X is more pronounced at lower pH values than at higher pH values. This observation is further supported by the fact that as pH increases, $1/\tau_{1f}$ decreases, whereas $1/\tau_{2f}$ increases. Since these relaxation rate constants are the aggregates of the various microscopic parameters, they do not report on the specific effects of pH on the individual kinetic or thermodynamic parameters of the underlying kinetic model. Such information is extracted from the IPCoA/IACoA concentration dependent relaxation studies at different pH values. We have previously elaborated on the determination of the individual kinetic/thermodynamic parameters for the MCAD-catalyzed reductive half-reaction at pH 7.6, essentially according to a theoretical (two-step) model of Strickland et al. (1975). Since a qualitatively similar dependence of the relaxation rate constants on IPCoA/IACoA concentrations has been observed at other pH values (Table 1), we have adopted the same analytical protocol. To comprehend the effect of pH on the microscopic parameters of the MCAD-catalyzed reductive half-reaction, let us review our previously proposed kinetic model for this enzyme (eq 3):

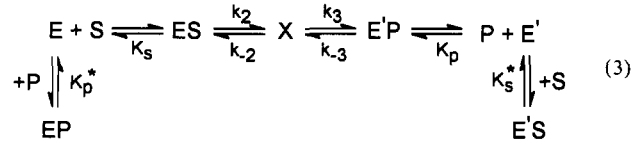

(3)

where E and E′ refer to MCAD–FAD and MCAD–$FADH_2$, respectively, and S and P refer to IPCoA and IACoA, respectively. This model is similar to that proposed by Schopfer et al. (1988) involving butyryl-CoA as the enzyme substrate. As discussed previously, the origin of the second relaxation step ($1/\tau_2$) in both forward and reverse directions lies in the formation of E′S and EP complexes, respectively. Given that $1/\tau_{1f} \gg 1/\tau_{2f}$ (at pH 6.4 and 7.6) and that $1/\tau_{1r} \gg 1/\tau_{2r}$ (at all pH's), the underlying steps can be considered to be uncoupled (Bernasconi, 1976). Hence, in accord with our earlier analysis, the relationships between the macroscopic rate constants (Table 1) and the microscopic parameters of eq 3 can be given as follows:

$$1/\tau_{1f(max)} = k_2 + k_{-2}; \quad 1/\tau_{1f(min)} = 1/\tau_{2r(min)} = k_{-2}$$

$$1/\tau_{2f(min)} = 1/\tau_{1r(min)} = k_3; \quad 1/\tau_{1r(max)} = k_3 + k_{-3}$$

$$K_{0.5(IPCoA)} = K_s; \quad K_{0.5(IACoA)} = K_p$$

On the basis of these relationships, we could translate the macroscopic rate constants of Table 1 into the microscopic parameters (Table 3) at pH 6.4 and 7.6. However, this approach could not be employed for the data at pH 9.0. This is because, due to comparable magnitudes of $1/\tau_{1f}$ and $1/\tau_{2f}$ at pH 9.0, the steps intrinsic to these relaxation rate constants could not be treated as uncoupled. Under this situation recourse was made to the numerical simulation for the model of eq 3 at pH 9.0, as described by Johnson and Srivastava (1993). The corresponding microscopic parameters at pH 9.0 are summarized in Table 3.

A close perusal of the data of Table 3 suggests that although the dissociation constant of the E–FAD–IPCoA complex is not affected within the pH range between 6.4 and 9.0, the dissociation constant of the E–$FADH_2$–IACoA complex varies by a factor of 4. At this time, we are uncertain whether this variation is real or is merely due to our inability to precisely determine $K_{0.5}$ values. However, from the data of Table 3, it is clear that as the pH increases, k_2 decreases, whereas k_{-2} increases. On the other hand, as pH increases, both k_3 and k_{-3} increase. This pattern can easily account for a higher amplitude of X at pH 6.4 than at pH 9.0 (see Figures 1 and 2).

The fact that k_3 of eq 3 (the rate constant for the decay of X) and the k_{cat} for the oxidase reaction both increase with an increase in the pH of the buffer media attests to our earlier proposition that the MCAD-catalyzed oxidase reaction might be limited by the rate of the decay of X. Since the increase in pH also increases k_{-3} (albeit not by an equal magnitude), it follows that the pH-dependent increase in $1/\tau_{2f}$ must be steeper than that of k_3. This is presumably the reason that the pH-dependent oxidase activity and $1/\tau_{2f}$ yield different pK_a values.

Can we predict the steady-state kinetic parameters for the oxidase reaction from the microscopic rate constants presented in Table 3? For making such a prediction, it is important to consider at what intermediary enzyme species the reduced flavin is oxidized by O_2. Clearly, the reduced flavin present in X is not oxidized by O_2, since the oxidation reaction is limited by the rate of collapse of X. Thus, either E–$FADH_2$ or its complex with IPCoA/IACoA is likely to be the target of the oxidation reaction. However, on the basis of X-ray crystallographic data (Kim et al., 1993) that the binding of fatty acyl-CoA's with MCAD "desolvates" the enzyme site environment, we consider the likely enzyme site for the oxidation of the reduced flavin to be E–$FADH_2$. This allows

us to propose the following steady-state kinetic scheme for the MCAD-catalyzed oxidase reaction (eq 4).

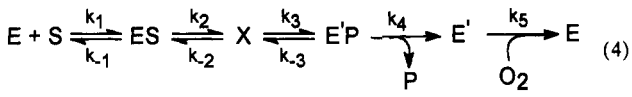

(4)

In this scheme, the last two steps are taken to be irreversible. The first irreversible step satisfies the condition of the initial rate measurements (i.e., when product is zero). The irreversibility of the second step is naturally justified since the electron transfer from E–$FADH_2$ to O_2 is a thermodynamically favorable reaction (Walsh, 1979). It is interesting to note that the rate of oxidation of MCAD–$FADH_2$ by O_2 (240 μM) remains unaffected over the pH range 6.4–9.0 (Table 3). The steady-state rate equation derived for the kinetic scheme of eq 4 provides relationships between the steady-state kinetic parameters (K_m for IPCoA and k_{cat}) for the oxidase reaction and the microscopic rate constants of eq 3:

$$K_m(\text{IPCoA}) = \frac{k_5\{k_3k_4(k_{-1} + k_2) + k_{-1}k_{-2}(k_{-3} + k_4)\}}{k_1\{k_4k_5(k_2 + k_{-2} + k_3) + k_{-3}k_5(k_2 + k_{-2}) + k_2k_3(k_4 + k_5)\}} \quad (5A)$$

$$k_{cat} = \frac{k_2k_3k_4k_5}{k_2k_3(k_4 + k_5) + k_{-3}k_5(k_2 + k_{-2}) + k_4k_5(k_2 + k_{-2} + k_3)} \quad (5B)$$

For predicting these steady-state kinetic parameters, the dissociation constant parameters K_s and K_p (of Table 1) were translated into the corresponding "on" and "off" rate constants on the assumption that the former is a diffusion-limited process (1×10^8 M^{-1} s^{-1}; Hammes, 1982). On this basis, the off rates (e.g., k_{-1} and k_4) are calculated from the dissociation constants of the E–FAD–IPCoA (K_s) and E–$FADH_2$–IACoA (K_p) complexes. Given these, as well as the microscopic parameters of Table 3, we could predict K_m for IPCoA and k_{cat} for the oxidase reaction at pH values 6.4, 7.6, and 9.0. These results are summarized, along with the experimentally determined parameters, in Table 2. The data of Table 2 show that both experimentally determined and predicted steady-state kinetic parameters increase with the increase in the pH of the buffer media. However, while the experimentally determined k_{cat}'s are more or less similar to those predicted at the corresponding pH values, K_m's for IPCoA under these conditions differ by a factor of 3–4. This variation is not significant in the light of the following two facts: (1) The experimentally determined K_m for IPCoA is in the sub-micromolar range at all pH values, and thus despite our effort to determine this parameter as carefully as possible, some variations can be expected. (2) The prediction of the steady-state kinetic parameters involves a complex function of the microscopic parameters, which have been determined by independent methods; thus, even small errors in these parameters can be expected to be amplified while predicting the steady-state kinetic parameters by eqs 5A and 5B. In the light of these considerations, the experimentally determined and predicted steady state kinetic parameters for the MCAD-catalyzed reaction can be taken to be remarkably similar.

On compilation of all of the experimental data presented herein, it is evident that both the substrate (IPCoA) and the pH of the buffer media serve as effectors of the MCAD-catalyzed oxidase reaction. Both of these effectors promote the oxidase activity by perturbing the equilibrium between X and the E–$FADH_2$–IACoA species such that the latter is favored. The substrate (IPCoA) accomplishes this task (rather indirectly) by combining with the E–$FADH_2$ form of the enzyme (Johnson & Srivastava, 1993), whereas the higher pH performs this function by destabilizing the electronic structure of IACoA within X such that the equilibrium distribution of this species (X) is favored toward both the E–FAD–IPCoA and E–$FADH_2$–IACoA complexes. Such an effect of pH is similar to that observed by us for the interaction of E–FAD with IACoA (Johnson et al., 1992). In this way, the effect of higher pH in promoting the oxidase activity of the enzyme is merely a happenstance, since pH promotes equilibration of X toward the E–$FADH_2$–IACoA species (responsible for the origin of the oxidase activity of the enzyme). The effect of higher pH on favorable equilibration of X toward the E–FAD–IPCoA complex is not realized in this regard. However, the latter effect becomes explicit as the K_m for IPCoA, during the dehydrogenation reaction, increases from 6.1 (pH 6.4) to 32.0 (pH 9.5; our unpublished results). We are currently testing our mechanistic principles, presented herein, for the origin of the oxidase activity involving different acyl-CoA substrates, including those (e.g., octanoyl-CoA) which are known to resist this activity, and we will report these findings subsequently.

REFERENCES

Beinert, H. (1963) *The Enzymes* (Boyer, P. D., Lardy, H., & Myrbach, K., Eds.) Vol. 7, pp 447–473, Academic Press, New York.

Bernasconi, C. F. (1976) *Relaxation Kinetics*, Academic Press, New York.

Crane, F. L., & Beinert, H. (1956) *J. Biol. Chem. 219*, 717–731.

Engel, P. C. (1990) *Chemistry and Biochemistry of Flavoenzymes* (Muller, F., Ed.) Vol. III, pp 597–655, CRC Press, Inc., London.

Frerman, F. E., Miziorko, H. M., & Beckman, J. D. (1980) *J. Biol. Chem. 255*, 11192–11198.

Ghisla, G., & Massey, V. (1989) *Eur. J. Biochem. 181*, 1–17.

Ghisla, S., Thorpe, C., & Massey, V. (1984) *Biochemistry 23*, 3154–3161.

Hammes, G. G. (1982) *Enzyme Catalysis and Regulation*, Academic Press, New York.

Johnson, J. K., & Srivastava, D. K. (1993) *Biochemistry 32*, 8004–8013.

Johnson, J. K., Wang, Z. X., & Srivastava, D. K. (1992) *Biochemistry 31*, 10564–10575.

Johnson, J. K., Kumar, N. R., & Srivastava, D. K. (1993) *Biochemistry 32*,11575–11585.

Kim, J. P., Wang, M., & Paschke, R. (1993) *Proc. Natl. Acad. Sci. U.S.A. 90*, 7523–7527.

Lau, S. M., Brantley, R. K., & Thorpe, C. (1989) *Biochemistry 28*, 8255–8262.

Lehman, T. C., Hale, D. E., Bhala, A., & Thorpe, C. (1990) *Anal. Biochem. 186*, 280–284.

McFarland, J. T., Lee, M., Reinsch, J., & Raven, W. (1982) *Biochemistry 21*, 1224–1229.

Nishino, T., Nishino, T., Schopfer, L. M., & Massey, V. (1989) *J. Biol. Chem. 264*, 2518–2527.

Schopfer, L. M., Massey, V., Ghisla, S., & Thorpe, C. (1988) *Biochemistry 27*, 6599–6611.

Strickland, S., Palmer, G., & Massey, V. (1975) *J. Biol. Chem. 250*, 4048–4052.

Thorpe, C., Matthews, R. G., & Williams, C. H., Jr. (1979) *Biochemistry 18*, 331–337.

Vanhove, G., Veldhoven, P. P. V., Eyssen, H. J., & Mannaerts, G. P. (1993) *Biochem. J. 292*, 23–30.

Walsh, C. (1979) *Enzymatic Reaction Mechanisms*, W. H. Freeman and Company, New York.

Wang, R., & Thorpe, C. (1991) *Biochemistry 30*, 7895–7901.